



This is a repository copy of *The accuracy of NMR protein structures in the Protein Data Bank*.

White Rose Research Online URL for this paper:
<https://eprints.whiterose.ac.uk/183017/>

Version: Accepted Version

Article:

Fowler, N.J. orcid.org/0000-0002-6005-935X, Sijoka, A. and Williamson, M.P. orcid.org/0000-0001-5572-1903 (2021) The accuracy of NMR protein structures in the Protein Data Bank. *Structure*, 29 (12). 1430-1439.e2. ISSN 0969-2126

<https://doi.org/10.1016/j.str.2021.07.001>

Article available under the terms of the CC-BY-NC-ND licence
(<https://creativecommons.org/licenses/by-nc-nd/4.0/>).

Reuse

This article is distributed under the terms of the Creative Commons Attribution-NonCommercial-NoDerivs (CC BY-NC-ND) licence. This licence only allows you to download this work and share it with others as long as you credit the authors, but you can't change the article in any way or use it commercially. More information and the full terms of the licence here: <https://creativecommons.org/licenses/>

Takedown

If you consider content in White Rose Research Online to be in breach of UK law, please notify us by emailing eprints@whiterose.ac.uk including the URL of the record and the reason for the withdrawal request.



eprints@whiterose.ac.uk
<https://eprints.whiterose.ac.uk/>

The accuracy of NMR protein structures in the Protein Data Bank

Nicholas J. Fowler¹, Adnan Sljoka^{2,3} and Mike P. Williamson^{1,*}

¹Dept of Molecular Biology and Biotechnology, University of Sheffield, UK.

²RIKEN Center for Advanced Intelligence Project, RIKEN, 1-4-1 Nihombashi, Chuo-ku, Tokyo, 103-0027 Japan.

³Dept of Chemistry, University of Toronto, UTM, 3359 Mississauga Road North, Mississauga, ON, L5L 1C6, Canada.

*Correspondence: m.williamson@sheffield.ac.uk

ORCID: N.J.F. 0000-0002-6005-935X A.S. 0000-0002-2398-9523. M.P.W. 0000-0001-5572-1903

Short title: The accuracy of NMR structures in the PDB

Highlights

- We summarise the accuracy of 4742 NMR ensembles from the PDB
- Most NMR structures are floppier than the true solution structure
- NMR structure quality improved up till 2005 but has not improved significantly since
- NOE violations are a poor measure of accuracy; Ramachandran distribution is better

Summary

The program ANSURRE measures the accuracy of NMR structures, by comparing rigidity obtained from experimental backbone chemical shifts, and from structures. We report ANSURRE analysis of NMR ensembles within the Protein Data Bank (PDB). NMR structures have improved in accuracy up till about 2005, since when accuracy has been fairly constant. Most structures have accurate secondary structure, but are generally too floppy, particularly in loops. There is a need for more experimental restraints in loops. The best current measures of accuracy are Ramachandran distribution and the number of NOE restraints per residue. The precision of structures within the ensemble correlates fairly well with accuracy, as does the number of hydrogen bond restraints per residue. If a structure contains additional components (such as additional polypeptide chains or ligands), then inclusion of these improves the accuracy of the structure. Analysis of over 7000 PDB NMR ensembles is available via our website ansurr.com.

Key words: NMR; protein structure; rigidity; experimental restraints; validation

INTRODUCTION

The accuracy of a protein structure describes how well the structure corresponds to the “true” time-dependent structure in solution. We recently described a method, ANSURRE (Accuracy of NMR Structures using Random Coil Index and Rigidity), which characterises the accuracy of NMR protein structures (Fowler et al., 2020). The method compares two measures of local rigidity: the *random coil index* (RCI), which uses backbone chemical shifts to estimate the fraction of random coil by residue (Berjanskii and Wishart, 2008), and *rigidity theory*, which takes the structure, converts it to a constraint graph, and calculates rigidity using a pebble-game algorithm, based on the program Floppy Inclusions and Rigid Substructure Topography (FIRST) (Jacobs et al., 2001). RCI is not a perfect experimental measure of local rigidity because it provides only a single value per amino acid residue,

43 but has the merits of being well understood and readily calculated. RCI and FIRST are compared
44 directly after re-scaling of RCI to ensure comparability, to generate scores measuring the accuracy of
45 the structure, as described below. In our description of the method (Fowler et al., 2020), we
46 compared ANSURRE scores to a range of other measures that might be expected to provide a
47 measure of accuracy, and also used the scores to provide a preliminary assessment of how NMR
48 structures compare to X-ray crystal structures. These comparisons were carried out on a manually
49 curated set of structures. In this work, we have expanded the comparison to study the accuracy and
50 quality of all NMR structures within the PDB that match our selection criteria.

51 Ways of estimating the accuracy of NMR structures have been investigated previously (Brünger et
52 al., 1993; Clore et al., 1993; Doreleijers et al., 1998; Huang et al., 2012; Snyder et al., 2005; Spronk et
53 al., 2004; Vranken, 2014; Williamson et al., 1995; Zhao and Jardetzky, 1994), including by a validation
54 task force set up by the PDB (Montelione et al., 2013). These measures can be divided into two
55 groups: *geometrical tests* and *comparisons to input data*. The geometrical tests are the same as
56 those used as validation measures by X-ray crystallography and electron microscopy, and include
57 measures of the proportion of residues within allowed or disallowed regions of the Ramachandran
58 plot, atomic clashes, and packing density. These are robust and reliable measures, but are aimed at
59 testing whether the protein structure has geometry that matches that obtained from high-quality
60 experimental structures, rather than whether it matches well to the NMR input data. The refinement
61 of NMR structures relies heavily on the quality of geometrical terms and force fields; much more
62 than does X-ray structure refinement, because NMR structure calculations have far fewer
63 experimental restraints. It is therefore reasonable to expect that geometrical tests should provide a
64 guide to the accuracy of NMR structures, and indeed this was shown in our preliminary comparisons,
65 where we found that the single best existing predictor of accuracy was the Ramachandran
66 distribution: either the proportion of residues in the allowed region or the proportion in the
67 disallowed region, which are strongly related. Nevertheless, it is clear that geometrical tests are not
68 in themselves measures of accuracy.

69 The more interesting set of tests are the comparisons to input data, since these should more clearly
70 discriminate the accuracy of structures. Crystallographers use the *R* factor, which directly compares
71 the experimentally determined electron density with the density predicted by the structure. NMR
72 spectroscopists have no equivalent measure. The most obvious equivalent is violations of NOE
73 restraints, or possibly the number of NOE restraints per residue. The biggest challenge in using these
74 as measures of accuracy is that NOE restraints are several removes from any experimental
75 measurement. The experimental measurement is the NOESY spectrum. To extract restraints from
76 the NOESY spectrum, the peaks must be picked: a person or a computer algorithm must decide
77 which peaks are noise or experimental artifacts, and which intensities are distorted by peak overlap
78 or baseline problems. There has to be a conversion from peak intensity (height or volume – not the
79 same thing, though both are problematic in different ways) to distance. Classically this is done using
80 a strong/medium/weak classification (Wüthrich, 1986), which avoids problems arising from
81 unknown amounts of internal motion in the protein, but is a rather subjective system. The distances
82 arising from this process are then fed into the structure calculation. This is an iterative process,
83 mainly because most chemical shifts can be assigned to more than one nucleus, and so most NOE
84 peaks are ambiguous, in the sense that a peak in the NOESY spectrum often cannot be assigned to a
85 unique pair of protons, but rather a set of possible pairs. Structure calculations therefore iteratively
86 reduce the ambiguity of existing restraints and possibly modify or add to the list of restraints. There
87 is also typically a process of checking and possibly removing restraints that are repeatedly violated in
88 structure calculations (Güntert, 2003). There is no theoretical justification for such an action, other
89 than the observation that some errors in NOE assignment are inevitable because of incomplete

90 knowledge. Another problem with NOE restraints is that they are usually applied as flat-well
91 potentials, implying that restraint violation distributions are not realistic (Bernard et al., 2011). A
92 final problem is that the best determined NOEs are the least useful, because they are typically
93 between protons that are within the same amino acid residue. Some practitioners often leave out
94 such NOEs because they have no information content, while others leave them in. Most NOEs in
95 multidimensional spectra occur in more than one location within the spectrum: practitioners differ
96 in whether only one or both such occurrences are used. Thus even such a fundamental measure as
97 the number of NOE restraints is not well defined. All of this means that comparisons to input data,
98 such as NOE restraint violations or numbers of restraints per residue, are ill-defined and handled
99 differently by different practitioners.

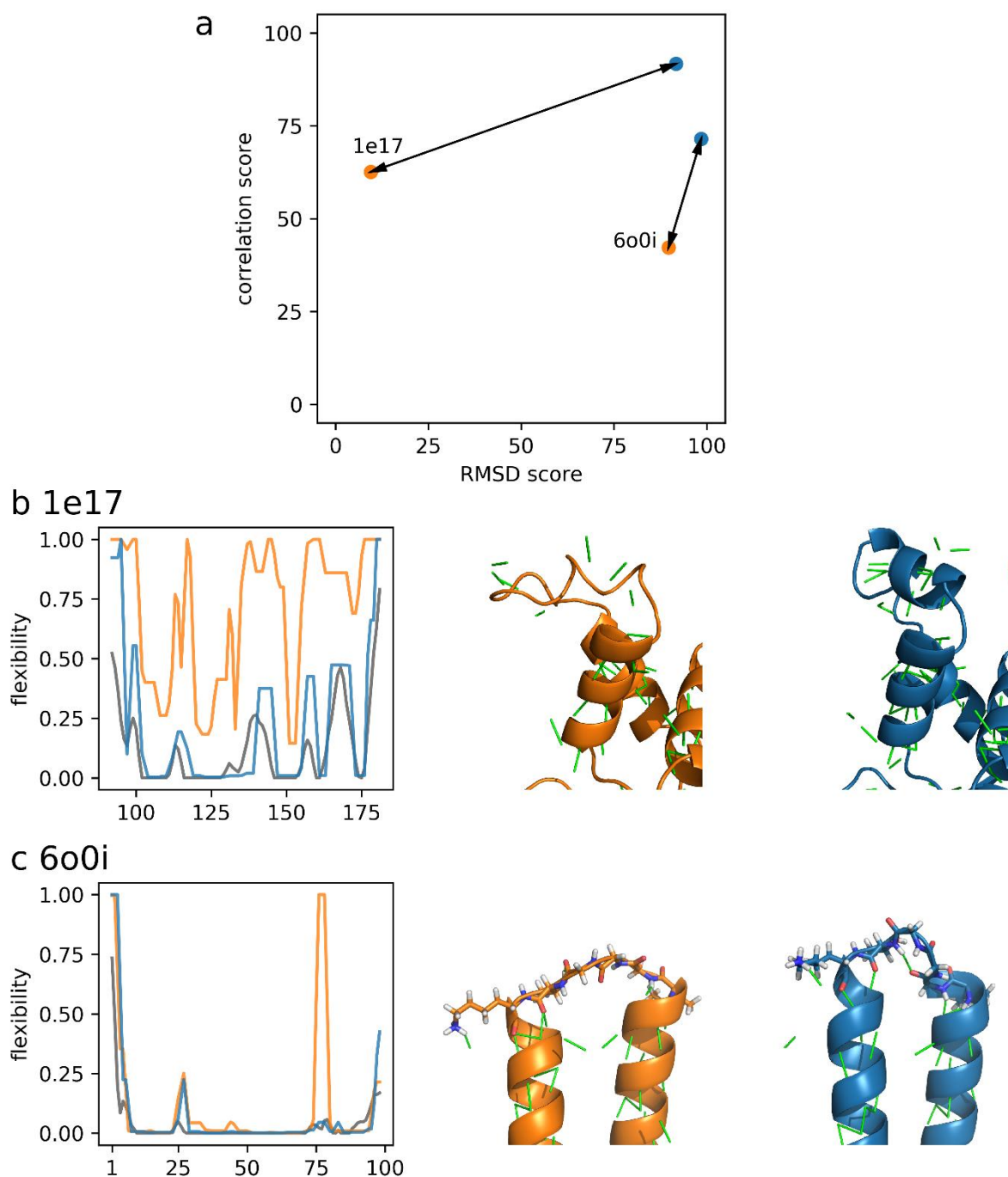
100 ANSURR provides a different type of validation, based on chemical shifts rather than distance
101 restraints. Backbone chemical shifts can often be obtained almost automatically from spectra and
102 are generally reliable. They are also easily available for any proteins with NMR structures, not least
103 because it is a requirement of PDB that chemical shift assignments be deposited with
104 BioMagResBank (BMRB) at the same time as structure deposition with PDB. This makes them good
105 parameters for validation.

106 In this paper, we explore what ANSURR can tell us about the accuracy of NMR structures in the PDB,
107 and conclude that although some structures are excellent, they vary considerably in their accuracy.
108 Following a general survey of PDB structures, we look at the different measures of structure quality,
109 to evaluate what they can tell us about structure quality. Finally, we look at the accuracy of
110 oligomers and complexes, and show that inclusion of all molecular components is beneficial to the
111 accuracy.

112 **RESULTS**

113 We noted previously (Fowler et al., 2020) that RCI is only reliable when the chemical shift
114 completeness of backbone shifts (HN, N, C α , C β , H α , C') is at least 75%. We have therefore used all
115 PDB (Berman et al., 2000) NMR structures for which a BMRB (Ulrich et al., 2008) chemical shift
116 assignment file exists at 75% completeness or more, and where the polypeptide chain is at least 20
117 residues long. This results in a subset of PDB structures, here named PDB75, which contains 4742
118 ensembles. Further details can be found in Methods.

119 ANSURR performs two different comparisons (Fig. 1): (1) The *correlation* between the rigidity
120 computed from chemical shifts (RCI) and from the structure using rigidity theory (FIRST). This
121 compares the overall shapes of the RCI and FIRST profiles, by testing whether peaks and troughs in
122 the two measures are in the same places. Because a peak is a locally flexible region (typically a loop)
123 and a trough is a locally rigid region (typically a region of regular secondary structure), this measure
124 is largely detecting whether secondary structure is correct. It is however rather more subtle than a
125 simple comparison of locations of secondary structure in that it includes a comparison of breaks and
126 weaknesses in secondary structure. (2) The root-mean-square-deviation (RMSD) between the RCI
127 and FIRST outputs. This measures the difference between the RCI and FIRST values for each residue
128 and thus tests whether the overall rigidity of the structure matches the rigidity as defined by RCI. An
129 important determinant of local rigidity is the presence of nonbonded interactions i.e. hydrogen
130 bonds and hydrophobic contacts. This comparison is thus to a large extent a measure of whether the
131 structure is close enough to the correct structure for nonbonded interactions to be formed correctly.
132 The two comparisons measure different aspects of the structure and are therefore not strongly
133 correlated.

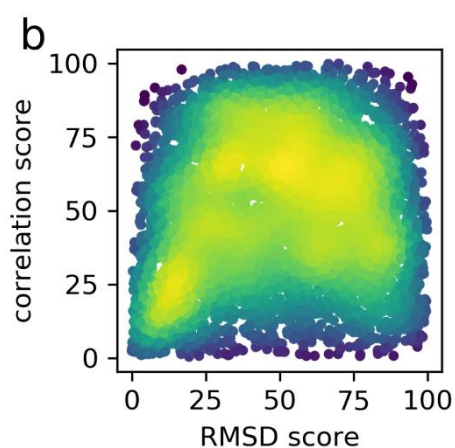
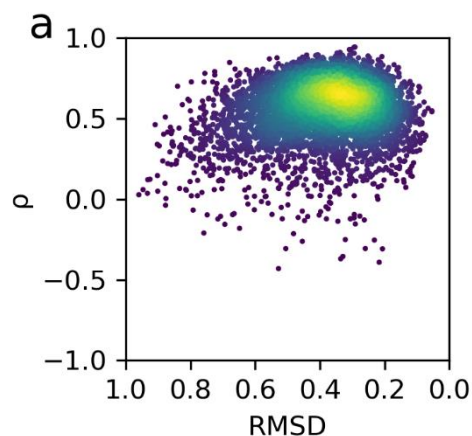


135

136 Figure 1. Outline of ANSRR output. (a) ANSRR compares measures of local rigidity produced from chemical
 137 shifts (RCI) and from the structure according to rigidity theory (FIRST). Two comparisons are made, namely the
 138 Spearman rank correlation, which largely determines whether peaks and troughs are in the same places; and
 139 the RMSD, which compares overall rigidities. The raw values are converted into scores, which are rank
 140 percentile values relative to all NMR protein structures in the PDB75 dataset (see Figure 2). These two scores
 141 can be visualised by plotting both on a 2-dimensional plot so that the best scoring structures will appear in the
 142 top right corner. Here, ANSRR scores are shown this way for two models of the DNA-binding domain of the
 143 human Forkhead transcription factor AFX (PDB ID 1e17) and two models of the designed protein XAA (PDB ID
 144 6o0i). (b) The flexibility computed for model 17 of 1e17 taken from the RECOORD16 (Nederveen et al., 2005)
 145 CNS [refined in vacuo (orange)] and CNW [refined in explicit solvent (blue)] datasets. RCI values are in grey. The
 146 CNW structure is more accurate, as measured by both correlation and RMSD scores. Middle and right: Residues
 147 120-140 of the CNS and CNW structures, respectively. Hydrogen bonds are indicated by green lines. Drastically

148 improved ANSURR scores, mostly RMSD score, are observed following refinement in explicit solvent. This
149 largely originates from the increased accuracy of nonbonded interactions (hydrogen bonds and hydrophobic
150 contacts). (c) Left: ANSURR analysis of chain A from model 7 (orange) and model 2 419 (blue) of the designed
151 protein XAA (PDB ID 6o0i). RCI values are in grey. The small loop between residues 74-79 in model 7 is too
152 floppy but correctly rigid in model 2, resulting in a better correlation score for model 2 (a). Middle and right:
153 The loop of models 7 and 2, respectively. The rigidity of the loop in model 2 is determined by a single hydrogen
154 bond which is not present in model 7, suggesting that the loop in model 7 is not representative of the solution
155 structure.
156

157 We have carried out ANSURR analyses of all 4742 NMR ensembles in the PDB75 dataset. These
158 analyses are available from our website ansurr.com. In Fig. 2a we present the average correlation
159 and RMSD values for each ensemble, shown as a two-dimensional plot. Poor structures are found in
160 the lower left corner, while good structures are in the upper right corner of such a plot. Structures
161 span a wide range of accuracy, with some very poor structures. Conversely, a significant number of
162 structures are of very good accuracy. The most densely populated region has a Spearman's rank
163 correlation coefficient ρ of around 0.7, indicating that most NMR structures in PDB75 have
164 essentially the correct secondary structure. The most common RMSD value is however only around
165 0.3, indicating that the structures have overall rigidity that does not match RCI well. In almost all
166 cases, the rigidity of the structure is lower than the rigidity implied by RCI, ie NMR structures are too
167 floppy. For most NMR structures, the rigidity in secondary structures is good, and the floppiness is
168 mainly in the loops (compare the two-dimensional plots on the left of Fig. 1b,c, where the troughs
169 have rigidities close to zero on both measures, and therefore match well, while the peaks are more
170 variable). Those who determine NMR structures have tended to concentrate on secondary structure
171 and not worried too much about loops, the general feeling being that loops are probably fairly
172 undefined in solution anyway, so that the lack of definition in loops (ie the spread of structures
173 within an ensemble) is probably "real". Our analysis indicates that this is not true – structures in
174 solution are considerably more structured and defined in loops than they are in typical NMR PDB
175 structures. For example, compare the loops in Fig. 1c, where addition of a single hydrogen bond
176 results in a large improvement in accuracy. We suggest that this represents a failing in many NMR
177 structures.



178

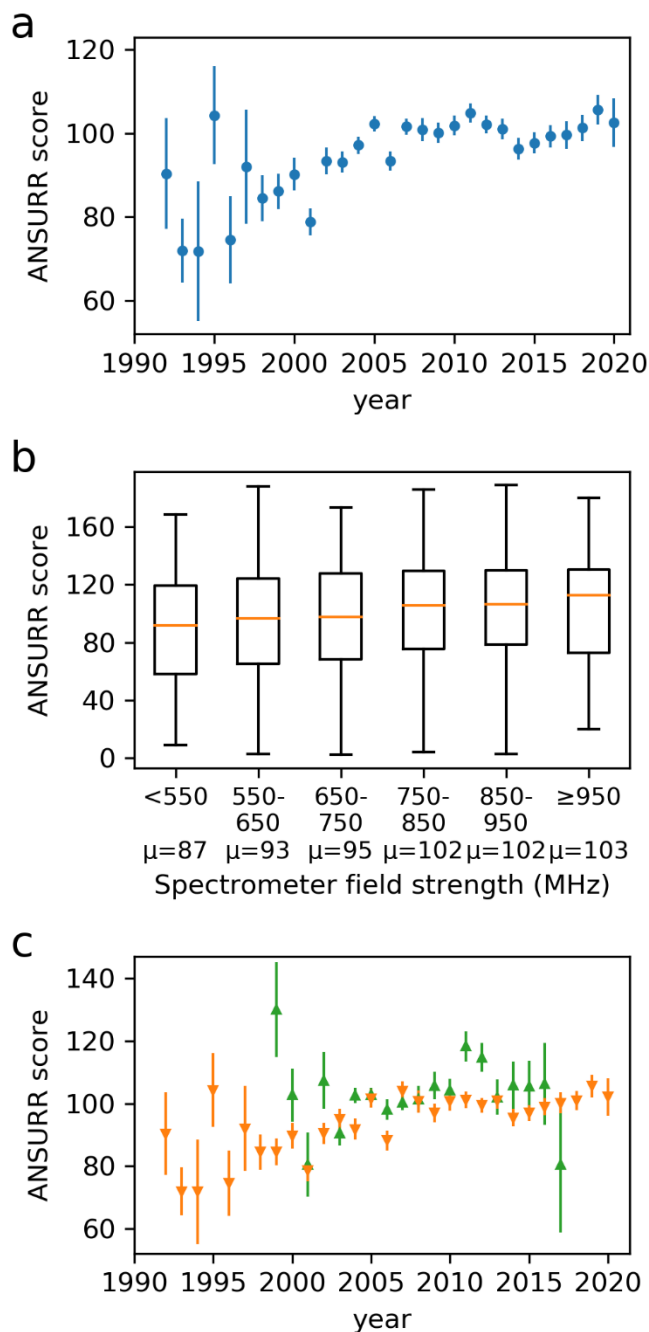
179 **Figure 2. Distribution of ANSURR measures from the PDB75 dataset.** For each ensemble in the
 180 dataset, we display the mean values for the ensemble rather than individual scores. (a) Raw values
 181 for correlation and RMSD. Note that that the RMSD values are displayed on a descending scale, for
 182 ease of comparison to scores. (b) The raw values have been convertible to percentile rank scores,
 183 which range from 0 (the worst structure in the PDB75) to 100 (the best). Colours represent the
 184 density of values.

185

186 The data in Fig 2a are nonlinear, making it difficult to judge by how much any individual ensemble is
 187 better or worse than typical PDB results. An alternative presentation of these data is thus to show
 188 the results as a percentile of the complete PDB75 dataset. We term these percentile values the
 189 correlation score and RMSD score, which by definition run from 0 to 100, and are summarised in Fig.
 190 2b. An advantage of the percentile scores is that the distributions of RMSD and correlation scores
 191 are more comparable, meaning that the correlation and RMSD scores can be summed to give an
 192 overall ANSURR quality score that measures the overall structural accuracy reasonably well, whereas
 193 the same cannot be said of the correlation and RMSD values themselves. In the subsequent analysis,
 194 we therefore add the correlation and RMSD scores together to produce a single accuracy score,
 195 termed ANSURR score, when it makes sense to use a single overall measure. The individual results
 196 for RMSD and correlation scores are shown in supplementary information.

197 **Accuracy has not improved significantly since 2005**

198 In our previous study (Fowler et al., 2020) we noted that a critical factor in improving accuracy was
 199 refinement in explicit solvent, which increased the ANSURR score by approximately 35. In this study
 200 we were unable to carry out such a comparison, because we were unable to work out, either from
 201 the PDB header or even from original publications in many cases, whether and how such refinement
 202 had been carried out. This further highlights the importance of reporting guidelines for PDB
 203 depositions. As a proxy, we looked at the relationship between ANSURR score and year of deposition
 204 (Fig 3a).



205
 206 **Figure 3. Trends in NMR accuracy with time.** (a) ANSURR score (sum of correlation and RMSD
 207 scores) for PDB75 NMR ensembles, as a function of year of deposition. Data are mean \pm standard
 208 error of the mean. Data points are plotted only for years with at least 3 ensembles from the PDB75
 209 dataset. (b) ANSURR score vs highest field strength cited in the PDB header. Data are shown as box
 210 plots, and indicate the median (orange lines), first and third quartiles (box) and extremes. Mean

211 values are indicated below the plot. (c) ANSURR score vs year of deposition. This shows the same
212 data as in (a) but split into structures coming from structural genomics consortia (green) and all
213 others (orange). Sample sizes for each plot are provided in supplementary information (SI Table 1).

214 It is clear that there was a gradual increase in accuracy with time, up to about 2005, after which
215 there is little obvious improvement. It is probably significant that the key papers on refinement in
216 explicit solvent were published in 2003 (Linge et al., 2003a; Linge et al., 2003b), and many of the
217 standard methods for calculating NMR structures (eg TALOS for dihedral restraints (Cornilescu et al.,
218 1999), CYANA (Güntert, 2004), XPLOR-NIH (Schwieters et al., 2003)) were also established in 2003 or
219 shortly before. Since then, there have been no step changes in the way protein NMR structures were
220 calculated. We hope that the results shown here will stimulate interest in improving the quality of
221 NMR structures.

222 There are several confounding factors that may also contribute to the improvement in structural
223 accuracy with time. One is the steady improvement in spectrometer sensitivity, largely from
224 increasing commercially available field strength, which will improve structural accuracy by providing
225 higher sensitivity and thus more complete NOE restraints. The results of this analysis are shown in
226 Fig 3b, which show that field strength has a significant effect on accuracy.

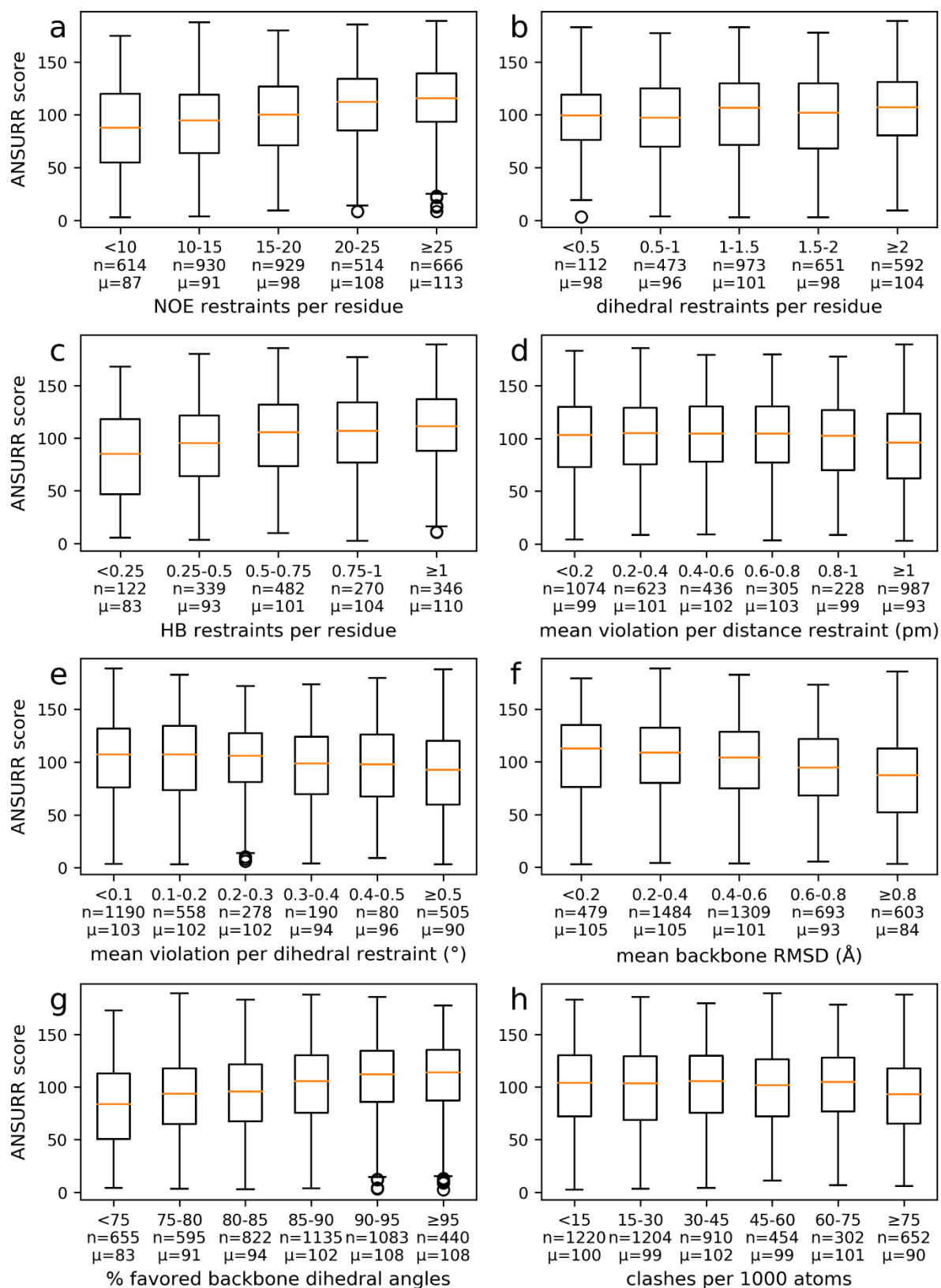
227 We also looked to see if specific research groups did noticeably well or badly in terms of accuracy.
228 There are too few structures from any individual group to produce useful conclusions, but we were
229 able to compare the accuracy of structures originating from structural genomics consortia to all
230 other structures (consortia are listed in SI Table 2). The results are shown in Fig 3c, and suggest that
231 structural genomics consortia have tended to generate slightly more accurate structures, though the
232 differences are small. It is worth noting that structural genomics consortia have also tended to focus
233 on “low-hanging fruit”, which yield good NMR spectra, and therefore might be expected to be more
234 accurate for that reason.

235 The trends with time are more apparent if we consider ANSURR scores obtained for all structures
236 regardless of backbone chemical shift completeness (SI Fig2). One would hope that this is because
237 we have better statistics with more structures, but these results must be interpreted with caution as
238 the accuracy of RCI is less reliable when chemical shift completeness is below 75%.

239 **NOE violations are a poor measure, though number of NOEs is good**

240 In our earlier study (Fowler et al., 2020) we looked at the correlation between ANSURR scores and a
241 range of quality measures typically used to characterise NMR protein structures. In that study we
242 used a set of 173 ensembles that had been processed and refined in a consistent way, with manually
243 curated checks on input restraints (Nederveen et al., 2005). Here we carry out a similar analysis, but
244 using all ensembles from the PDB75 dataset. It is a much larger dataset, but also a much less uniform
245 one. For simplicity, we present here summed ANSURR scores, discussing the component correlation
246 and RMSD scores where relevant. RMSD and correlation scores plotted separately are provided in
247 supplementary information (SI Fig3).

248 There is a strong relationship between ANSURR score and the number of NOE restraints per residue
249 (Fig 4a). We noted in the Introduction that there is a lack of consistency among NMR practitioners in
250 the counting of NOE restraints, but this does not hide the expected influence of number of NOEs on
251 accuracy. The effect is seen almost entirely on RMSD score rather than correlation score (see SI
252 Fig3a); in other words, increased numbers of NOE restraints help tie down local structure better,
253 rather than improving the definition of secondary structure.



254

255 **Figure 4. Dependence of ANSURR scores on other measures of structural accuracy.** Data are
 256 presented as in Fig 3b, as box plots. The number of samples and the mean are indicated below each
 257 box. (a) Number of NOE restraints per residue. (b) Number of dihedral restraints per residue. (c)
 258 Number of hydrogen bond restraints per residue. (d) Mean size of distance restraint violation (Å). (e)
 259 Mean size of dihedral restraint violation (°). (f) Mean backbone root-mean-square-difference (RMSD)

260 – the precision). (g) Percentage of backbone (ϕ , ψ) pairs within the favoured regions of the
261 Ramachandran plot, as measured by MolProbity. (h) Clashscore (clashes per 1000 atoms), as
262 measured by MolProbity.

263 By contrast, the relationship between the number of dihedral restraints per residue and ANSRR
264 score is less apparent (Fig 4b). Nonetheless, structures with at least two dihedral restraints per
265 residue (mean ANSRR score of 104) tend to score better than those with zero (mean ANSRR score
266 of 97, two-sided *t*-test *p*-value = 1.4×10^{-5}). If we consider RMSD and correlation scores separately (SI
267 Fig3b), we see that RMSD score increases with the density of dihedral restraints, but at the expense
268 of correlation score. This suggests that dihedral restraints act to rigidify a structure by improving
269 backbone geometry but are perhaps too weak to improve the overall accuracy significantly.

270 There is a strong relationship between ANSRR score and the number of hydrogen bond restraints
271 per residue (Fig 4c). This relationship arises entirely from the RMSD score (SI Fig3c), and shows that
272 NMR structures have greatly improved rigidity when hydrogen bond restraints are present. This
273 effect is most noticeable in loops, which in NMR structures are generally too floppy in comparison to
274 the RCI values. In crystal structures, there are usually hydrogen bonds that serve to rigidify the
275 structure, and our results indicate that such hydrogen bonds are retained in solution, since adding
276 them produces structures that match well to RCI values (to be published). In the absence of
277 hydrogen bond restraints, much of the hydrogen bonding network will be determined by the
278 forcefield used during refinement. However, the forcefield alone is clearly unable to induce
279 hydrogen bonds when they are not present in the unrefined structure. There is thus a clear
280 implication: NMR structures will be greatly improved in their overall accuracy (particularly in the
281 loops) if we can find experimental restraints that define the hydrogen bonds. To date the only
282 reliable hydrogen bond restraint comes from $^3\text{H}_{\text{NC}}$ scalar couplings, usually obtained from long-range
283 HNC0 spectra (Cordier and Grzesiek, 1999). Such couplings are small, and typically only observable
284 for small proteins with long relaxation times. There is therefore a challenge for NMR, to identify
285 suitable hydrogen bond restraints that can be used to improve structures.

286 Neither distance nor angle violations particularly correlate with ANSRR score, although structures
287 with higher level of violations ($>0.01 \text{ \AA}$ per distance restraint, $>0.3^\circ$ per dihedral restraint) tend to
288 score slightly worse (Fig 4d, e). This suggests that violations can help to diagnose structures with
289 significant errors but may not be a useful guide to accuracy. It is worth repeating the comments
290 made above, that in many structure calculations, restraints that are repeatedly violated are omitted
291 or modified in subsequent iterations, implying that violation statistics may not be reliable guides to
292 accuracy (Gronwald and Kalbitzer, 2004; Herrmann et al., 2002; Xu et al., 2001).

293 There is a moderate relationship between the ANSRR score and the backbone RMSD between
294 structures in the ensemble (the precision of the ensemble; Fig 4f). In other words, the accuracy and
295 precision of the ensemble are related: more accurate ensembles also have tighter precision. This
296 finding is different from what we saw previously with a manually curated set of structures (Fowler et
297 al., 2020), where there was very little correlation between accuracy and precision, though it matches
298 some earlier studies of the relationship between accuracy and precision (Clare and Gronenborn,
299 1998). We hypothesise that in structure calculations where the NOE network is sufficiently dense to
300 limit the precision effectively, the NOEs will also tend to improve the accuracy, but this merits
301 further investigation.

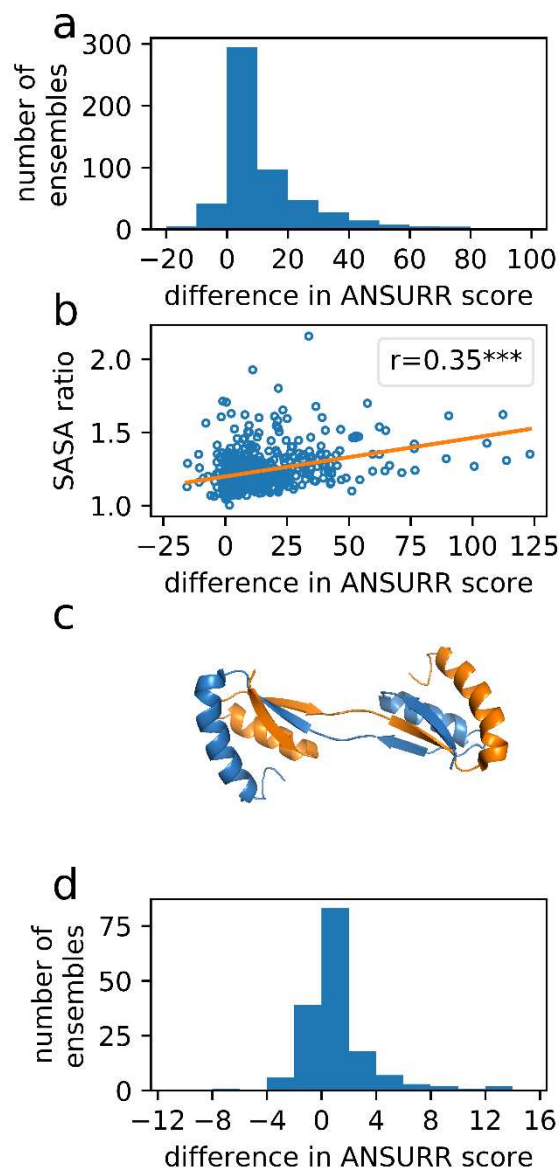
302 **The best existing measure is Ramachandran distribution**

303 There is a clear relationship between ANSURR score and the percentage of residues in the favoured
304 region of the Ramachandran plot (Fig 4g). The process of NMR structure determination is a joint
305 refinement against both the experimental restraints and knowledge-based parameters (van der
306 Waals packing, coulombic forces, bond/angle potentials, solvent interactions etc) and it is therefore
307 not a surprise that accurate structures should also have good Ramachandran distributions. On the
308 other hand, there is very little relationship with clashscore (Fig 4h). We saw a similar effect in our
309 previous study (Fowler et al., 2020).

310 **Inclusion of ligands improves the accuracy**

311 About 13% of NMR structures in the PDB comprise more than one polymer chain, ie are oligomers or
312 have bound peptides. It has been previously shown using X-ray crystal structures that interactions
313 between subchains can significantly affect the rigidity of biological assemblies as a whole
314 (Jagodzinski et al., 2013). Here we analyse ANSURR scores computed for 550 biological assemblies
315 that were calculated using NMR). Figure 5a shows the difference between the ANSURR score
316 obtained when rigidity is computed for the entire biological assembly and when rigidity is computed
317 for subchains individually. ANSURR score improves for 92% (504/550) of NMR ensembles when
318 rigidity is computed for the entire biological assembly. The results clearly demonstrate that the
319 formation of biological assemblies significantly affects rigidity and in a way that leads to better
320 agreement with rigidity calculated from chemical shifts. It might be expected that greater
321 improvements in ANSURR score would be seen for assemblies which share a larger degree of contact
322 between the constituent chains, and this is indeed the case. In figure 5b the ratio of the solvent
323 accessible surface area (SASA) summed over individual chains and that for the biological assembly
324 (assemblies with larger degree of contact between chains will have greater SASA ratios) is plotted
325 against the difference in ANSURR score. As an example, figure 5c shows the oligomer 2MJA for
326 which the ANSURR score increases by 90 when rigidity is computed for the entire assembly. It is easy
327 to see why. The structure is made up of beta strands formed by a combination of the two chains,
328 which when separated would become considerably more flexible (Whiteley, 2005).

329 About 15% of NMR protein structures contain non-polymer instances e.g. ligands such as drug
330 molecules and metals. We analysed ANSURR scores computed for 162 NMR ensembles with bound
331 ligands. Figure 5d shows the difference in ANSURR score obtained when rigidity is computed with
332 ligands present and without. ANSURR score improves for 57% of the ensembles, is unchanged for
333 15% of ensembles and is worse for 28% of ensembles. Overall, the total change in ANSURR score is
334 much less than in our biological assemblies analysis above. This is to be expected as bound ligands
335 are generally much smaller than polymer chains in biological assemblies and would be expected to
336 make much less difference to the total flexibility. Regardless, it seems that more often than not,
337 bound ligands do alter the rigidity of the structure, and in a way that tends to improve agreement
338 with rigidity calculated from chemical shifts.



339

340 **Figure 5. The effect of including other components in a biological assembly in the PDB75 dataset.**

341 (a) The change in ANSURR score when the entire multichain assembly is used for the ANSURR
 342 calculation, as opposed to calculating the scores for subchains independently. The mean change is
 343 12. (b) Weak but significant correlation (Pearson's $r=0.35$, two-tailed $p\text{-value}=7.8\times 10^{-18}$) between the
 344 ratio of solvent accessible surface area summed over individual chains and that for the biological
 345 assembly, and the difference in ANSURR score. (c) The structure of the protease GlpG (PDB 2MJA),
 346 which comprises a domain-swapped dimer, and has a large improvement in ANSURR score when
 347 rigidity is calculated for the dimer, compared to the two monomers separately. (d) The change in
 348 ANSURR score when adding non-peptide partners to the assembly, such as small molecule ligands
 349 and metals. The mean change is 1.

350

351

352

353

354 **DISCUSSION**

355 We report on the application of the method ANSURR, which measures the accuracy of NMR protein
356 structures. Previous methods for assessment of accuracy have relied either on analysis of NOE
357 violations, or on the precision of the ensemble. Both of these are poorer measures of accuracy, for
358 reasons discussed here. Our method compares the rigidity of the structure to the rigidity indicated
359 using a modified version of the random coil index, and thus provides a measure of accuracy that
360 compares experimental measurements to the final structure. The method has been applied to all
361 NMR ensembles in the PDB that have chemical shift data in BMRB. The analysis presented here has
362 focused on ensembles with at least 75% backbone chemical shift completeness and at least 20
363 amino acid residues, but can be applied to any NMR structure. Our website ansurr.com provides
364 details for all PDB NMR structures with chemical shifts in the BMRB, with warnings for those
365 ensembles calculated with less than 75% chemical shift completeness.

366 ANSURR scores can be calculated rapidly and easily for any NMR protein structure, and (with the
367 help of the underlying data, Fig. 1) provide a simple and user-friendly measure of accuracy. The PDB
368 currently provides a slider bar assessment of structure quality for each deposited ensemble, which
369 focuses on geometrical quality rather than accuracy. ANSURR provides a general measure of
370 accuracy for NMR protein structures, which we hope will be useful for the structural biology
371 community. A majority of the users of PDB are not depositors, and are thus not 'structural biology
372 experts' but scientists looking for the insight that can be provided by structural details. For such
373 users, NMR structures have been problematic because it has been unclear how accurate they are,
374 and therefore whether NMR structures can be used with the same confidence that (for example)
375 crystal structures can. ANSURR goes at least some way to answering this problem, by providing a
376 measure of accuracy that does not rely on NOE restraints.

377 The analysis provided here shows that there is a large range in the accuracy of NMR structures in the
378 PDB. Structure calculation improved steadily up to about 2005, since when there has been little
379 change in overall accuracy. The majority of structures have good correlation between rigidity
380 calculated from chemical shifts and from the structure, indicating that the regular secondary
381 structure is generally correct. Our previous paper (Fowler et al., 2020) made a comparison between
382 NMR structures and crystal structures, within a limited number of curated structures, and showed
383 that from correlation scores, the secondary structure of NMR and crystal structures are of
384 comparable accuracy.

385 However, the same cannot be said for RMSD score. Our analysis shows that the large majority of
386 NMR structures are too floppy, by comparison to the "true" rigidity indicated by RCI. This applies
387 throughout the structures, but because regular secondary structure is inherently fairly rigid, it is
388 more evident, and more troubling, in loops. Structural biologists tend to compare structures by
389 overlaying them for best fit over backbone atoms, and then displaying them as cartoon plots, which
390 emphasise the locations and orientation of regular secondary structure elements. This is a sensible
391 practice, but it leads to the widespread assumption that the important features of a protein are its
392 regular secondary structure, and that loops are relatively unimportant. Indeed, at least among the
393 NMR community, there is a general feeling that loops in solution are probably not well defined, and
394 that the variability seen in loops (and differences in loops between NMR structures and crystal
395 structures) reflect the "real" flexibility of loops and are not a major cause for concern. Our analysis
396 shows this is not true: most loops in solution are much less flexible than is indicated by the
397 ensemble, and loops in NMR structures are for the most part underdetermined and inaccurate. A
398 recent publication (Juárez-Jiménez et al., 2020) reaches similar conclusions, using different
399 methodology. This is a consequence of the fact that there are usually very few NOE restraints in

400 loops, and often very few restraints at all. Our analysis implies that NMR spectroscopists need to
401 work harder to identify structural restraints within loops, because this will significantly improve the
402 overall accuracy of the structures. Methods for the identification of hydrogen bonds would be of
403 particular importance, because of the power of hydrogen bonds to limit flexibility. There are several
404 other methods of refinement that could be useful for restricting loops, including residual dipolar
405 couplings (Prestegard et al., 2004), application of a conformational database (Kuszewski et al., 1996)
406 and restraints on the radius of gyration (Kuszewski et al., 1999).

407 Here, we have compared ANSURRE scores to a range of parameters that might be considered to
408 provide a measure of accuracy. We have shown that the distribution of backbone dihedral angles
409 within the Ramachandran surface is a good measure of accuracy (Fig. 4g), as are the number of NOE
410 restraints (Fig. 4a) and the number of hydrogen bond restraints (Fig. 4c). We tried to make
411 comparisons with other factors, in particular the method of structure refinement (for example,
412 inclusion of explicit solvent) and the programs and parameters used for structure calculation and
413 refinement, but were unable to do so, because the PDB record fields do not hold this information in
414 a consistent way, and we were unable to come up with a machine-readable way of getting the
415 information. Indeed in many cases it is not possible to be confident what the authors did even from
416 reading the relevant papers. There is thus a need to generate more consistent and machine-readable
417 documentation of the methodology used to calculate NMR structures. We note that PDB and BMRB
418 are discussing the introduction of a NMR Exchange Format which could help to improve such
419 documentation (Gutmanas et al., 2015).

420 The results presented here make it clear that there remains considerable scope for improving the
421 accuracy of NMR structures, particularly in loops, which is where most ligand binding sites and
422 enzyme active sites are located (Papaleo et al., 2016; Wierenga, 2001). Better measures of accuracy
423 are likely to drive better accuracy, which can only benefit the entire community.

424 **STAR★METHODS**

425 Detailed methods are provided in the online version of this paper and include the following:

426 KEY RESOURCES TABLE

427 RESOURCE AVAILABILITY

428 METHOD DETAILS

429 QUANTIFICATION AND STATISTICAL DETAILS

430 **SUPPLEMENTAL INFORMATION**

431 Supplemental information can be found online at xxxx

432 **ACKNOWLEDGEMENTS**

433 We thank the Biotechnology and Biological Science Research Council (BBSRC) for funding to N. J. F.
434 (BB/P020038/1), and CREST, Japan Science and Technology Agency (JST) and PRISM for funding to A.
435 S.

436 **AUTHOR CONTRIBUTIONS**

437 Conceptualization, N.J.F. and M.P.W.; Investigations, N.J.F.; Analysis, N.J.F., A.S. and M.P.W.; Writing,
438 N.J.F., A.S. and M.P.W.; Funding Acquisition, M.P.W.

439 **DECLARATION OF INTERESTS**

440 Authors declare no competing interests.

441 **Data availability:**

442 All study data are provided in the Supplementary Information. In addition, ANSURRE scores for 7187
443 NMR protein structures can be viewed and downloaded from our website ansurr.com.

444 Data deposition: The ANSURRE program and associated documentation can be downloaded from
445 github.com/nickjf/ANSURRE, <https://doi.org/10.5281/zenodo.416158660>. A typical calculation on an
446 ensemble of 20 models for a 150-residue protein takes less than a minute. ANSURRE output for all
447 PDB ensembles can be found on ansurr.com.

448 **STAR★METHODS**

449 **KEY RESOURCES TABLE**

REAGENT or RESOURCE		
Deposited Data		
Protein data bank	(Berman et al., 2000)	www.rcsb.org
NMR restraints grid	(Doreleijers et al., 2005)	restraintsgrid.bmrblib.org
RECOORD	(Nederveen et al., 2005)	https://www.ebi.ac.uk/pdbe/recalculated-nmr-data
BMRB	(Ulrich et al., 2008)	https://bmrblib.org/
Software and Algorithms		
ANSURRE	(Fowler et al., 2020)	www.ansurr.com
Molprobit	(Chen et al., 2010)	http://molprobit.biochem.duke.edu/
PyMol molecular graphics system	Schrödinger, LLC	https://pymol.org/2/

450

451 **RESOURCE AVAILABILITY**

452 **Lead contact**

453 Further information and requests for information on method, dataset or computational resources
454 should be directed to and will be fulfilled by the Lead Contact, Prof. M. P. Williamson
455 (m.williamson@sheffield.ac.uk).

456 **Materials availability**

457 No new unique reagents or materials were produced in this study.

458 **Data and code availability**

459 The PDB codes used can be accessed from PDB, and BMRB codes from BMRB. The ANSURRE program
460 is available for download from github.com/nickjf/ANSURRE, DOI 10.5281/zenodo.4161586.

461 **EXPERIMENTAL MODEL AND SUBJECT DETAILS**

462 Not applicable.

463 **METHOD DETAILS**

464 ***ANSURRE calculations***

465 7187 NMR protein structure ensembles and their corresponding backbone chemical shifts were
466 downloaded from the PDB and BMRB, respectively. Paired PDB and BMRB IDs are provided as a
467 supplementary text file (pdb_chain_bmr.txt). ANSURRE was used to validate each model in each
468 NMR ensemble with the following options: re-reference chemical shifts using PANAV, include non-
469 standard residues, include ligands and combine chains when computing flexibility. As the number of
470 models in an ensemble varies (from a single model to hundreds), we averaged the correlation, RMSD
471 and ANSURRE scores for all members of each ensemble. Scores for each model are provided as a
472 supplementary text file (ansurr_scores_Nov2020.out) and can also be downloaded from our website
473 ansurr.com. Unless stated otherwise, the analysis in this work was performed on the subset of
474 ensembles with at least 20 residues and at least 75% chemical shift completeness. This subset is
475 termed PDB75 and comprises 4742 ensembles.

476 ***Established data-driven quality measures***

477 The quality measures used in our analysis presented in figure 4 were generated as follows. The
478 number of restraints per residue and the mean restraint violations per residue were acquired from
479 the NMR Restraints Grid restraintsgrid.bmr.wisc.edu (Doreleijers et al., 2003; Doreleijers et al.,
480 2005). Mean backbone RMSDs were extracted from PDB validation reports for each ensemble with
481 more than 1 model. The average percentage of favoured backbone dihedral angles was computed
482 for each ensemble using the program ramalyze, part of the Molprobit suite (Chen et al., 2010). The
483 program clashscore (also part of Molprobit) was used to compute the average number of clashes
484 per 1000 atoms for each ensemble.

485 ***Dataset of oligomeric NMR protein structures***

486 The PDB was searched for oligomeric NMR protein structures using the advanced search function on
487 the RCSB PDB website (www.rcsb.org). This set of structures was then filtered to include only those
488 which had a corresponding set of backbone chemical shifts on the BMRB with at least 75% chemical
489 shift completeness and had at least 20 residues in each chain. The final set comprised 550 protein
490 NMR structures. ANSURRE scores when rigidity is computed for the entire biological assembly are
491 provided in ansurr_scores_Nov2020.out. ANSURRE scores when rigidity is computed separately for
492 each subchain are provided as a supplementary text file (ansurr_scores_asmonomers.txt)

493 ***Dataset of NMR protein structures containing free ligands***

494 The advanced search function on the RCSB PDB website was used to obtain NMR protein structures
495 that contained at least one non-polymer instance. An in-house program was used to exclude
496 structures with ligands which contained metals because the strength of bonds which include metals
497 cannot be determined from a protein structure without further calculations e.g. with density
498 functional theory or quantum mechanics. This set was then filtered to include only those which had
499 a corresponding set of backbone chemical shifts in the BMRB with at least 75% chemical shift
500 completeness and had at least 20 residues in each chain. The final set comprised 162 protein NMR
501 structures. ANSURRE scores when rigidity is computed with ligands included are provided in
502 ansurr_scores_Nov2020.out. ANSURRE scores when rigidity is computed without ligands included are
503 provided as a supplementary text file (ansurr_scores_noligands.txt).

504 **QUANTIFICATION AND STATISTICAL ANALYSIS**

505 Statistical analyses were performed using standard Python routines.

506 **References**

507 Berjanskii, M.V., and Wishart, D.S. (2008). Application of the random coil index to studying protein
508 flexibility. *Journal of Biomolecular NMR* *40*, 31-48.

509 Berman, H.M., Westbrook, J., Feng, Z., Gilliland, G., Bhat, T.N., Weissig, H., Shindyalov, I.N., and
510 Bourne, P.E. (2000). The Protein Data Bank. *Nucleic Acids Res.* *28*, 235-242.

511 Bernard, A., Vranken, W.F., Bardiaux, B., Nilges, M., and Malliavin, T.E. (2011). Bayesian estimation
512 of NMR restraint potential and weight: A validation on a representative set of protein structures.
513 *Proteins-Structure Function and Bioinformatics* *79*, 1525-1537.

514 Brünger, A.T., Clore, G.M., Gronenborn, A.M., Saffrich, R., and Nilges, M. (1993). Assessing the
515 quality of solution nuclear magnetic resonance structures by complete cross-validation. *Science* *261*,
516 328-331.

517 Chen, V.B., Arendall, W.B., III, Headd, J.J., Keedy, D.A., Immormino, R.M., Kapral, G.J., Murray, L.W.,
518 Richardson, J.S., and Richardson, D.C. (2010). MolProbity: all-atom structure validation for
519 macromolecular crystallography. *Acta Crystallographica Section D-Structural Biology* *66*, 12-21.

520 Clore, G.M., and Gronenborn, A.M. (1998). New methods of structure refinement for
521 macromolecular structure determination by NMR. *Proceedings of the National Academy of Sciences*
522 *of the United States of America* *95*, 5891-5898.

523 Clore, G.M., Robien, M.A., and Gronenborn, A.M. (1993). Exploring the limits of precision and
524 accuracy of protein structures determined by nuclear magnetic resonance spectroscopy. *Journal of*
525 *Molecular Biology* *231*, 82-102.

526 Cordier, F., and Grzesiek, S. (1999). Direct observation of hydrogen bonds in proteins by interresidue
527 $^3\text{H}_{\text{NC}}$ scalar couplings. *Journal of the American Chemical Society* *121*, 1601-1602.

528 Cornilescu, G., Delaglio, F., and Bax, A. (1999). Protein backbone angle restraints from searching a
529 database for chemical shift and sequence homology. *Journal of Biomolecular NMR* *13*, 289-302.

530 Doreleijers, J.F., Mading, S., Maziuk, D., Sojourner, K., Yin, L., Zhu, J., Markley, J.L., and Ulrich, E.L.
531 (2003). BioMagResBank database with sets of experimental NMR constraints corresponding to the
532 structures of over 1400 biomolecules deposited in the Protein Data Bank. *J. Biomol. NMR* *26*, 139-
533 146.

534 Doreleijers, J.F., Nederveen, A.J., Vranken, W., Lin, J.D., Bonvin, A.M.J.J., Kaptein, R., Markley, J.L.,
535 and Ulrich, E.L. (2005). BioMagResBank databases DOCR and FRED containing converted and filtered
536 sets of experimental NMR restraints and coordinates from over 500 protein PDB structures. *J.*
537 *Biomol. NMR* *32*, 1-12.

538 Doreleijers, J.F., Rullmann, J.A.C., and Kaptein, R. (1998). Quality assessment of NMR structures: a
539 statistical survey. *Journal of Molecular Biology* *281*, 149-164.

540 Fowler, N.J., Sljoka, A., and Williamson, M.P. (2020). A method for validating the accuracy of NMR
541 protein structures. *Nature Communications* *11*, 6321.

542 Gronwald, W., and Kalbitzer, H.R. (2004). Automated structure determination of proteins by NMR
543 spectroscopy. *Progress in Nuclear Magnetic Resonance Spectroscopy* *44*, 33-96.

544 Güntert, P. (2003). Automated NMR protein structure calculation. *Progress in Nuclear Magnetic*
545 *Resonance Spectroscopy* *43*, 105-125.

546 Güntert, P. (2004). Automated NMR structure calculation with CYANA. *Methods in molecular biology*
547 (Clifton, N.J.) *278*, 353-378.

548 Gutmanas, A., Adams, P.D., Bardiaux, B., Berman, H.M., Case, D.A., Fogh, R.H., Güntert, P.,
549 Hendrickx, P.M.S., Herrmann, T., Kleywegt, G.J., *et al.* (2015). NMR Exchange Format: a unified and
550 open standard for representation of NMR restraint data. *Nature Struct. Mol. Biol.* *22*, 433-434.

551 Herrmann, T., Güntert, P., and Wüthrich, K. (2002). Protein NMR structure determination with
552 automated NOE assignment using the new software CANDID and the torsion angle dynamics
553 algorithm DYANA. *Journal of Molecular Biology* *319*, 209-227.

554 Huang, Y.J., Rosato, A., Singh, G., and Montelione, G.T. (2012). RPF: a quality assessment tool for
555 protein NMR structures. *Nucleic Acids Research* *40*, W542-W546.

556 Jacobs, D.J., Rader, A.J., Kuhn, L.A., and Thorpe, M.F. (2001). Protein flexibility predictions using
557 graph theory. *Proteins-Structure Function and Genetics* *44*, 150-165.

558 Jagodzinski, F., Clark, P., Grant, J., Liu, T., Monastra, S., and Streinu, I. (2013). Rigidity analysis of
559 protein biological assemblies and periodic crystal structures. *Bmc Bioinformatics* *14*, S2.

560 Juárez-Jiménez, J., Gupta, A.A., Karunanithy, G., Mey, A.S.J.S., Georgiou, C., Ioannidis, H., De Simone,
561 A., Barlow, P.N., Hulme, A.N., Walkinshaw, M.D., *et al.* (2020). Dynamic design: manipulation of
562 millisecond timescale motions on the energy landscape of cyclophilin A. *Chemical Science* *11*, 2670-
563 2680.

564 Kuszewski, J., Gronenborn, A.M., and Clore, G.M. (1996). Improving the quality of NMR and
565 crystallographic protein structures by means of a conformational database potential derived from
566 structure databases. *Protein Science* *5*, 1067-1080.

567 Kuszewski, J., Gronenborn, A.M., and Clore, G.M. (1999). Improving the packing and accuracy of
568 NMR structures with a pseudopotential for the radius of gyration. *Journal of the American Chemical*
569 *Society* *121*, 2337-2338.

570 Linge, J.P., Habeck, M., Rieping, W., and Nilges, M. (2003a). ARIA: automated NOE assignment and
571 NMR structure calculation. *Bioinformatics* *19*, 315-316.

572 Linge, J.P., Williams, M.A., Spronk, C.A.E.M., Bonvin, A.M.J.J., and Nilges, M. (2003b). Refinement of
573 protein structures in explicit solvent. *Proteins: Structure Function and Bioinformatics* *50*, 496-506.

574 Montelione, G.T., Nilges, M., Bax, A., Guentert, P., Herrmann, T., Richardson, J.S., Schwieters, C.D.,
575 Vranken, W.F., Vuister, G.W., Wishart, D.S., *et al.* (2013). Recommendations of the wwPDB NMR
576 validation task force. *Structure* *21*, 1563-1570.

577 Nederveen, A.J., Doreleijers, J.F., Vranken, W., Miller, Z., Spronk, C.A.E.M., Nabuurs, S.B., Güntert, P.,
578 Livny, M., Markley, J.L., Nilges, M., *et al.* (2005). RECOORD: A recalculated coordinate database of
579 500+proteins from the PDB using restraints from the BioMagResBank. *Proteins: Structure Function*
580 *and Bioinformatics* *59*, 662-672.

581 Papaleo, E., Saladino, G., Lambrugh, M., Lindorff-Larsen, K., Gervasio, F.L., and Nussinov, R. (2016).
582 The role of protein loops and linkers in conformational dynamics and allostery. *Chem. Rev.* *116*,
583 6391-6423.

584 Prestegard, J.H., Bougault, C.M., and Kishore, A.I. (2004). Residual dipolar couplings in structure
585 determination of biomolecules. *Chemical Reviews* *104*, 3519-3540.

586 Schwieters, C.D., Kuszewski, J.J., Tjandra, N., and Clore, G.M. (2003). The XPLOR-NIH NMR molecular
587 structure determination package. *Journal of Magnetic Resonance* *160*, 65-73.

588 Snyder, D.A., Bhattacharya, A., Huang, Y.P.J., and Montelione, G.T. (2005). Assessing precision and
589 accuracy of protein structures derived from NMR data. *Proteins: Structure Function and*
590 *Bioinformatics* *59*, 655-661.

591 Spronk, C.A.E.M., Nabuurs, S.B., Krieger, E., Vriend, G., and Vuister, G.W. (2004). Validation of
592 protein structures derived by NMR spectroscopy. *Progress in Nuclear Magnetic Resonance*
593 *Spectroscopy* *45*, 315-337.

594 Ulrich, E.L., Akutsu, H., Doreleijers, J.F., Harano, Y., Ioannidis, Y.E., Lin, J., Livny, M., Mading, S.,
595 Maziuk, D., Miller, Z., *et al.* (2008). BioMagResBank. *Nucleic Acids Res.* *36*, D402-D408.

596 Vranken, W.F. (2014). NMR structure validation in relation to dynamics and structure determination.
597 *Progress in Nuclear Magnetic Resonance Spectroscopy* *82*, 27-38.

598 Whiteley, W. (2005). Counting out to the flexibility of molecules. *Physical Biology* *2*, S116-S126.

599 Wierenga, R.K. (2001). The TIM-barrel fold: a versatile framework for efficient enzymes. *FEBS Letts*
600 *492*, 193-198.

601 Williamson, M.P., Kikuchi, J., and Asakura, T. (1995). Application of ¹H NMR chemical shifts to
602 measure the quality of protein structures. *Journal of Molecular Biology* *247*, 541-546.

603 Wüthrich, K. (1986). *NMR of proteins and nucleic acids* (New York: Wiley).

604 Xu, Y., Jablonsky, M.J., Jackson, P.L., Braun, W., and Krishna, N.R. (2001). Automatic assignment of
605 NOESY cross peaks and determination of the protein structure of a new world scorpion neurotoxin
606 using NOAH/DIAMOD. *J. Magn. Reson.* *148*, 35-46.

607 Zhao, D.Q., and Jardetzky, O. (1994). An assessment of the precision and accuracy of protein
608 structures determined by NMR: Dependence on distance errors. *Journal of Molecular Biology* 239,
609 601-607.
610